Performance Analysis of FSO Communication Systems with Higher-Order Spatial Diversity Schemes Using BPSK-SIM over Log-Normal Atmospheric Turbulence Channels

Okikiade A. Layioye[1], Thomas J. O. Afullo[1], and Pius A. Owolawi[2]
[1] University of KwaZulu-Natal, Durban, 4001, South Africa
[2] Tshwane University of Technology, Pretoria, South Africa
Email: okiki.layioye@yahoo.com; afullot@ukzn.ac.za; p.owolawi@gmail.com

Abstract—Free Space Optical (FSO) communication system is an optical wireless connectivity operating at an unlicensed optical spectrum, with lots of advantages over the conventional Radio Frequency (RF) transmission. However, the performance of the FSO channel is limited due to atmospheric turbulence and severe weather conditions. There are many authors who have worked on mitigating these effects by using Spatial Diversity (SD) with 2X2-MIMO systems and few have worked up to 4X4-MIMO systems, blended with BPSK-Sub-carrier Intensity Modulation (BPSK-SIM) under the log-normal atmospheric turbulence model. However, in this paper, we extended the SD technique to higher-order configurations such as 8X8-MIMO system in order to improve the performance obtained from lower-order FSO systems. This study was considered at log-irradiance variance values of 0.1 and 0.9, representing the mildly weak and moderately weak atmospheric turbulence regimes respectively. This work has presented the performance analysis of various FSO-SD techniques. As a result, at BER of 10^{-9} the 1X8, 4X4, 6X6 and 8X8 higher-order SD systems were ≈46%, 55%, 61% and 69% respectively better than the "non-diversity" FSO system during the moderately weak atmospheric condition. Also, their channel capacities were ≈74%, 77%, 85% and 89% respectively better than the "non-diversity" FSO system at SNR of 30 dB.

Index Terms—Atmospheric turbulence, BPSK-Sub-Carrier intensity modulation, free space optical communication systems, higher-order spatial diversity technique, log-normal atmospheric turbulence model

I. Introduction

Free Space Optical (FSO) Communication System is an Optical Wireless Communication (OWC) system that can be described as a robust technology that provides users with a superior mobility, flexibility as well as high data rate. The FSO communication system conveys information by transmitting laser beams through the atmosphere to a photodetector. In the recent years, it has attracted applications in both indoor and outdoor wireless communications. It has proven to be a good and viable substitute to other traditional wireless communication systems due to its large bandwidth, easy deployment and commissioning, and cost effectiveness. The sophisticated outdoor wireless capabilities of the FSO system, with lots of other optimal services mentioned above are part of its advantages over other types of wireless communication systems. Based on its numerous and broad applications, the FSO communication system has attracted great attention and has become a widely used OWC system for the improvement of the Average Channel Capacity (ACC) of communication systems [1]-[5].

The motivation for alternative technology that meets today's wireless access platform is as a result of the last-mile bottleneck. This is coupled with continually increasing demand placed on the need for higher bandwidth and transmission rate, along with certain Radio Frequency (RF) limitations due to frequency spectrum congestion [1], [6], [7]. The FSO system has proved to be a communication system with allocation for high speed, broad (wide) bandwidth, interference-free, highly directional, reasonable security, license-free, robust communication services with less time of deployment and also importantly it has a low maintenance cost. Another advantage of the FSO is its ability to equal the speed of the Fiber optics, which is as high as 1.25 Gbps and as a matter of fact, it has the ability to surpass this speed to reach 10 Gbps. The reason being that it transmits data faster through air than in the glass fibers used in fiber optics [1], [8], [9].

However, the effects of the atmospheric conditions greatly determine the reliability and efficiency of the FSO communication system by causing a fluctuation in the irradiance of the optical signal which is known as atmospheric scintillation [10]-[12]. The main disadvantages of the FSO communication system arise from the occurrences associated with atmospheric conditions resulting into atmospheric turbulence or adverse weather conditions. The atmospheric turbulence effects are caused by the differences detected in the refractive index as a result of the in-homogeneities in temperature and also by fluctuations obtained in air pressure along the transmission pathway of the laser beam [4], [12], [13]. The effects of the index in-homogeneities obviously have a great deteriorating impact on the quality of the received signal and at the same time it can cause variations in both the received

Manuscript received May 25, 2017; revised July 13, 2017.
Corresponding author email: okiki.layioye@yahoo.com.
doi:10.12720/jcm.12.7.379-394

signals' intensity and phase. As a matter of fact, the long run effects of these variations can result into an increasing link error probability, thereby causing a limitation to the performance of the FSO communication system. These atmospheric turbulence conditions can be categorized into weak, intermediate and strong atmospheric turbulence regimes depending on the level of the atmospheric turbulence strength [4], [5], [12], [14]. The Received Optical Signal Level (ROSL) at the receiver can be adversely affected as a result of atmospheric disorders such as the occurrence of Fog and haze which leads to beam scattering, thereby reducing the ROSL. Also, the higher the magnitude of the fog, the higher the attenuation that it produces. Attenuation exceeding 300 dB/km is caused by heavy fog, which in turn limits the length of the FSO link to a range that is less than 100*m* [6], [15], [16]. The effects of some atmospheric conditions such as rain and snow are not quite harmful to FSO communication systems, but it has been observed that they mainly cause serious attenuation to the radio and microwave frequencies [6], [16], [17].

Overcoming the corruption effects on optical signals caused by fading that has been induced by turbulence can be achieved by several diversity techniques. The employment of different methods under the diversity techniques can be used to improve the channel performance of the FSO communication links. The conventional diversity techniques used in FSO communication system are space diversity, time diversity, wavelength diversity, frequency diversity and temporal diversity [18]-[20]. As sited by several authors, spatial diversity technique can be considered as a promising mitigating technique for FSO communication to produce a high data rate. This led to an investigation into the spatial correlation amongst a pair of configured transmitters in a Multiple Input Multiple Output (MIMO) structure as presented in [21]. However, the atmospheric effects are controllable and can be greatly minimized to a reasonable level through the use of the MIMO technique. This includes the application of multiple lasers at the transmitter end as well as multiple photodetectors at the receiver end [18], [22], [23]. Another work discussed the performance investigation of multi-beam Free Space Optical system using diversity techniques [24].

The choice of the appropriate modulation scheme to achieve an optimum FSO performance is a key factor in mitigating against the induced fading which is as a result of atmospheric turbulence. The modulation techniques that are the simplest as well as most extensively employed for FSO systems are the On-Off Keying (OOK) scheme and the Pulse Position Modulation (PPM) [6], [9], [13]. Though the OOK scheme has shown that it doesn't deliver any form of protection or resistance to induced fading caused by the atmospheric turbulence [4], [6], [14], [25]. The level of the optical intensity obtained at the position of the receiver sometimes experiences a random instability which is caused by the non-predictive behavior of the atmospheric turbulence level. Therefore, all these suggest that for the OOK technique to produce an optimum performance when it is applied, it will definitely need an adaptive thresholding scheme. However, due to the formation of this scheme, the implementation tends to be complex and practically not suitable [6], [17], [26]. Meanwhile, the PPM modulation technique on the other hand seems to have a poor bandwidth efficiency, despite its low cost and simplicity [13]. Applying the modulation schemes that convey the required information in either the frequency or the phase of the carrier signal has become a reasonable and better approach. This is because the level of the optical intensity in FSO communication system is drastically affected by fog and scintillation [6]. Therefore, following the trend of current researches, a proposition has been made that the limitations obtained from the employment of the OOK or PPM can be overcome by the employment of Sub-carrier (SC) Intensity Modulation (SIM) schemes. The various types of Sub-carrier Intensity Modulation schemes that can be applied are: Sub-carrier Binary Phase Shift Keying (SC-BPSK) and Sub-carrier Quadrature Amplitude Modulation (SC-QAM). However, this paper employed the former. As a matter of fact, the Binary Phase Shift Keying (BPSK) based SIM does not need any adaptive thresholding scheme and it is moderately bandwidth efficient. This makes it a better option when compared to the operations of the OOK and PPM in the presence of fading channels that have been induced by the atmospheric turbulence [14], [20], [27], [28]. Thus, a comprehensive investigation of the FSO communication system performance using SC-PSK has been shown in [17], [25], [28], [29], but without considering the spatial diversity technique. Wilson et al. in [30]-[32], considered the FSO MIMO communication system using the Pulse Position Modulation (PPM) and the Q-ary PPM under two turbulent induced fading channels which are: the log-normal and Rayleigh fading channels, and then made expressions and analysis on the Bit Error Probability (BER) and the Symbol Error Probability (SER).

Apart from the usual study of Average Bit Error Rate (ABER) and Average Symbol Error Rate (ASER) performance for MIMO-FSO communication systems, the average capacity performance of these systems are now recently studied in [13], [33]. The Average Channel Capacity (ACC) is also a standard metric system for determining the maximum possible data rate (in b/s/Hz) consistently transmitted between the transmit lasers and the receive photodetectors in the FSO communication regime [34]. In addition to the BER and the ACC performance analysis studied in this paper for higher-order spatial diversity FSO systems, the Outage Channel Capacities (OCC) of these FSO systems were also studied under the weak turbulence regime.

Thus, from the foregoing, the performance on the ACC of FSO-MIMO Communication systems under different atmospheric turbulence induced fading channels such as the weak, intermediate and strong atmospheric turbulence fading channels has not been fully investigated. This

work investigates the BPSK-SIM over MIMO and other Spatial Diversity (SD) techniques (such as Single Input Multiple Output (SIMO) and Multiple Input Single Output (MISO)); whereby the Subcarrier Intensity Modulation is employed to improve the capacity of the FSO system by making sure that the multiple sources are being modulated at different sub-carriers. Though, to obtain a preferred BER performance, the penalty that is paid is the higher SNR. Therefore, in situations whereby we place great priority on the increase in capacity of the system more than the power requirement, then it will be proper to choose the multiple SIM technique.

The arrangement of this paper is given as follows: Section 2 explains explicitly the system and channel models that were used in this work. The performance analysis showing the BER, ACC and OCC of the various higher-order spatial diversity schemes are presented in Section 3. Numerical results as well as the graphical analysis of the higher-order spatial diversity schemes under the mildly weak and moderately weak atmospheric turbulence regimes are shown in Section 4. Finally, the last section states the conclusion with remarks of this paper.

II. System and Channel Models

A. System Model

1) FSO-SISO systems using BPSK

The whole system model in this case involves the Free Space Optical SISO system using BPSK modulation technique with a structure that consists of a single transmitter at the input and a single receiver at the output of the optical link. This type of FSO system employs BPSK signaling to modulate the intensity of the optical signal produced by the single transmit laser by means of a carrier signal created by the modulator.

A simple block diagram to describe the Free Space Optical SISO system which uses the BPSK-SIM modulation technique is shown in Fig. 1. The source input data (d_i) which carries the information to be conveyed to a user at a distant destination, becomes modulated by the BPSK modulator onto the created RF subcarrier. It is then relayed onto a laser which is described as an optical carrier. The *g(t)* in the FSO SISO BPSK-SIM block diagram denotes the rectangular pulse shaping function of the BPSK modulator. In order to bias the optical carrier appropriately, the created complex RF signal is being mixed with a DC bias signal b_o. This synchronization ensures that the optical carrier totally accepts the full swing of the time varying RF subcarrier signal. Thus, after synchronization with the DC bias signal, the intensity of the optical source becomes modulated by the RF subcarrier. However, the modulated optical information produced by the laser is transmitted over the free space which is an atmospheric channel. The atmospheric channel considered in this paper is a weak turbulent regime. The log-normal distribution is used to model the weak turbulence effect which results into fading of the transferred optical signal intensity. Using a Coherent Detection (CD) technique at the receiver, we can conveniently recover the complex Sub-carrier Intensity Modulated signal that has been superimposed on the covering of the inbound optical signal. In order to capture the sub-carriers, the Electrical Bandpass filters are used. Following this is the standard RF coherent detector which is also the BPSK demodulator that, thus recovers the transferred data series given as D_i.

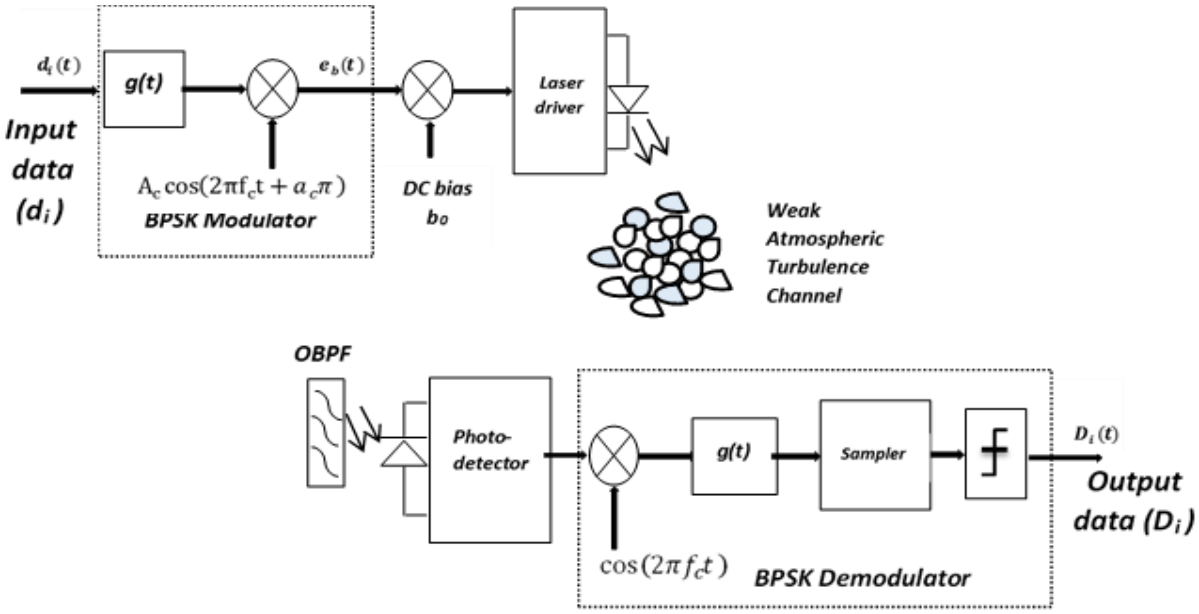

Fig. 1. The block diagram of BPSK sub-carrier intensity modulated SISO-FSO link under the log-normal atmospheric channel.

In this SISO case, a single RF sub-carrier that has BPSK sub-carrier amplitude, sub-carrier phase and sub-carrier frequency as A_c, a_c, and f_c is being used [6]. It is confirmed that as the photodetector (PD) optically detects

and collects optical signal at the receiver end, this process is done in the presence of the following: signal distortion, noise interference and background radiation [8]. The expression for the transmitted optical signal intensity from the single laser driver is expressed as [14]:

$$s(t) = P_a\{1 + \kappa e_b\} \quad (1)$$

where P_a represents the average optical signal power per bit and κ denotes the index of modulation which is given as $0 < \kappa \leq 1$. However, the Peak transmitted optical signal power (P_p) is related to the average optical signal power per bit as follows: $P_a = P_p / 2$.

The electrical BPSK sub-carrier signal $[e_b(t)]$ is given as [6], [25]:

$$e_b(t) = A_c g(t)\cos(2\pi f_c t + a_c \pi) \quad (2)$$

where *t* is the time in seconds and all other parameters remain as earlier described. Thus, (1) becomes:

$$s(t) = \frac{P_p}{2}\{1 + \kappa[A_c \cos(2\pi f_c t + a_c \pi)]\} \quad (3)$$

After modulation, the transmitted optical signal from the laser is transmitted over the atmospheric turbulence regime where it gets distorted by atmospheric effects, such as scintillation, fog, rain, snow and so on. Thus, in an FSO communication system with the effects of scintillation and the likes, the received optical signal intensity *r(t)* at the input of the single photodetector is given as [35]:

$$r(t) = aC(t)P_o(t) \quad (4)$$

In (4), parameter *a* denotes the atmospheric attenuation factor contributed by other effects rather than scintillation, *C(t)* is the signal scintillation factor due to the effects of the atmospheric turbulence, which can then be demonstrated as a stationary random process. $P_o(t)$ represents the received signal intensity without considering the effects of scintillation. However, it can be said that $s(t) = P_o(t)$.

Therefore, for BPSK systems in an FSO communication system, the received optical signal intensity at the input of the single photodetector is given as [14]:

$$r(t) = aC(t)s(t) \quad (5)$$

$$r(t) = aC(t)\frac{P_p}{2}\{1 + \kappa[A_c \cos(2\pi f_c t + a_c \pi)]\} \quad (6)$$

This received optical signal intensity has already been distorted while being transmitted over the atmospheric turbulence channel. Consequently, since we are considering the weak atmospheric turbulence channel in this paper, C(t) can be modelled with the Log-normal distribution as a stationary random process.

The mean amplitude $(aC(t)\frac{P_p}{2})$ of the received electrical signal which is also called the DC term of the signal can be filtered out using a bandpass filter, which is incorporated into the receiving end of the FSO system. Hence, at the output of the photodetector, after it has been filtered and converted from the optical form, we can obtain the expression for the electrical signal as follows [14].

$$r_e(t) = aC(t)\frac{P_p}{2}\Re\kappa e_b(t) + \nu(t) \quad (7)$$

$$r_e(t) = aC(t)\frac{P_p}{2}\Re\kappa A_c \cos(2\pi f_c t + a_c \pi) + \nu(t) \quad (8)$$

where $\Re$ is the Photodetector's responsivity; this is a parameter that gives the responsivity of the photodetector or how reactive the photodetector is. $\nu(t)$ represents the total receiver noise. This noise factor contributed or accumulated at the receiver can be modelled as an Additive White Gaussian Noise (AWGN) process which has a power spectral density N_0.

Finally, the received electrical signal undergoes BPSK demodulation and then afterwards becomes sampled in order to recover the original information (data). Hence, for the BPSK demodulation of the received electrical signal $r_e(t)$, the output signal $R(t)$ that contains the original data can be finally obtained after the received electrical signal $r_e(t)$ is demodulated by the reference signal $A_c \cos(2\pi f_c t)$ and given as [14]:

$$R(t) = r_e(t)A_c \cos(2\pi f_c t) \quad (9)$$

$$R(t) = aC(t)\frac{P_p}{2}\Re\kappa\frac{A_c}{2} + \nu(t) \quad (10)$$

Therefore, after the BPSK-SIM coherent detection demodulation, baseband electrical signal that will be obtained at the end of the FSO SISO communication link is given as [14], [35]:

$$R(t) = \frac{1}{4}aC(t)P_p\Re\kappa A_c + \nu(t) \quad (11)$$

2) FSO spatial diversity systems using BPSK

The Spatial Diversity technique involves employing multiple antennas on either the transmitter or receiver (MISO or SIMO respectively), or having more than one antenna on both the transmitter and receiver as in the case of MIMO. However, as shown in Fig. 2, a universal $M_T \times N_R$ FSO Diversity system using the BPSK-SIM modulation technique can be considered and deduced. Hence, this generic formulation can be used to handle the FSO-MISO, FSO-SIMO and FSO-MIMO systems.

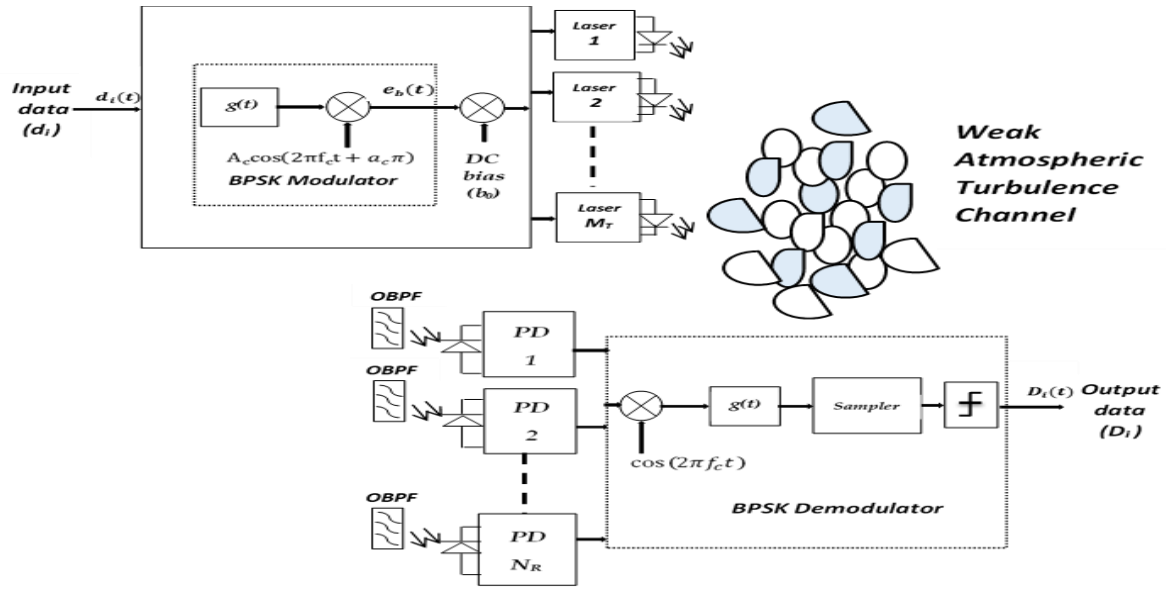

Fig. 2. The block diagram of BPSK sub-carrier intensity modulated spatial diversity FSO links under the log-normal atmospheric channel

In this paper, the systems described above employed BPSK signaling with a set of M_T transmitting lasers directed towards a set of aligned N_R receiving Photodetectors (PD). The M_T transmitting lasers individually provide an explicit perfect synchronized data transmission which employs similar BPSK signals. These data transmission, with seamless synchronization by each of the transmitting lasers, provide a stream of data transmitted through an atmospheric turbulence channel directed towards the N_R photodetectors at the receiving end. However, in order to justify the performance analysis, it is important to make certain assumptions such as assuming that each transmit telescope's light beam-width is sufficiently broad to make sure that the receiver array is being completely illuminated. Also, it is essential to include the assumption that irrespective of M_T, the same total optical power is being produced by the transmitter's telescope array. This is done in order to impose a reasonable evaluation with the case of a system having a single transmit telescope. The spatial correlation has to be insignificant when considering these spatial diversity techniques. Thus, for this to be negligible, it has to be assumed that the distance between the discrete transmit and receive telescopes is sufficient.

The model for the turbulence channels of the various Diversity systems can be represented by an atmospheric turbulence channel C, having an $M_T \times N_R$ matrix which describes the configurations of the Diversity turbulence channel, and it is given as [13], [14]:

$$C = [C_{mn}(t)]_{m,n=1}^{M_T,N_R} \tag{12}$$

However, at the input of the BPSK demodulator, the electrical signal is given as [13], [14]:

$$r_e(t) = [a][\frac{P_p}{2}][\Re][\kappa][e_b(t)]\sum_{m=1}^{M_T}\sum_{n=1}^{N_R} C_{mn}(t) + \nu(t) \tag{13}$$

m = 1, 2 …, M_T and n = 1, 2 …, N_R,

where $C_{mn}(t)$ represents the stationary random process which describes the atmospheric turbulence channel between the *mth* transmit laser to the *nth* photodetector, and $\nu(t)$ denotes the Additive White Gaussian Noise with zero mean and a noise power $N_0^{(n)}$.

The transmitted electrical signal can be estimated at the receiving end by employing the means of a Maximum Ratio Combining (MRC) Detector. The MRC was chosen in this paper due to the fact that in terms of optimum performance, it has a combining gain advantage which adds benefits to the FSO system. This is as a result of the fact that the required SNR expected to reach a certain BER performance is slightly lower for MRC compared to other combining schemes such as Equal Gain Combining (EGC) and Selection Combining (SC). Unlike other combiners, the MRC performs its operation by estimating the gains of all the channels of the diversity system. Therefore, as a result of this, a finite sum of the individual sub-channel Signal to Noise Ratios can be obtained. This respectively gives an expression for the Instantaneous Electrical SNR (IE-SNR), and it is given as follows [13], [14]:

$$\gamma = (\sum_{m=1}^{M_T}\sum_{n=1}^{N_R}\sqrt{\gamma_{mn}})^2 \tag{14}$$

$$\gamma = (\sum_{m=1}^{M_T}\sum_{n=1}^{N_R}\sqrt{\bar{\gamma}_{mn}}C_{mn})^2 \tag{15}$$

The factor γ_{mn} is obtained as Random Variables (RVs) of arbitrary sizes and it describes the component of the Instantaneous Electrical SNR. This component is caused by the signal that results from the sub-channel. Each of the sub-channels that exist from the mth transmit laser to the nth photodetector contributes to the Instantaneous Electrical SNR (IE-SNR). Thus, γ_{mn} is expressed as follows [13], [14]:

$$\gamma_{mn} = \frac{(\frac{1}{M_T N_R} C_{mn} a \Re P_a \kappa)^2}{N_0} = \bar{\gamma}_{mn} C^2{}_{mn} \quad (16)$$

where N_0 is a representation of the total noise power of the system. However, from a combination of the various instantaneous electrical SNR components obtained from the various sub-channels in the middle of the mth transmit laser and the nth photodetector, the average electrical SNR $(\bar{\gamma}_{mn})$ can be found and it is contributed by the various sub-channels. From (16), $\bar{\gamma}_{mn}$ is obtained as [13], [14]:

$$\bar{\gamma} = \frac{(\frac{1}{M_T N_R} a \Re P_a \kappa)^2}{N_0} \quad (17)$$

Hence, for FSO SISO communication system, the average electrical signal to noise ratio is given as:

$$\bar{\gamma} = \frac{(a \Re P_a \kappa)^2}{N_0} \quad (18)$$

(since m = n = 1, for SISO systems).

B. Channel Model

1) Atmospheric turbulence model

The irradiance fluctuations that arise in the FSO system as a result of certain atmospheric turbulence conditions within the link regime can be described using various statistical models. However, the irradiance fluctuations can be described in various levels based on the impact of the atmospheric turbulence. This has led to the fact that the atmospheric turbulence condition can be categorized as weak, intermediate (moderate) or strong turbulent conditions.

The atmospheric turbulence induced fading that describes perfectly the weak atmospheric turbulence condition used in this paper is expected to be a random process that has the same pattern like the log-normal distribution [13], [17]. On the other hand, the random process for the atmospheric turbulence induced fading for the intermediate and the strong turbulence conditions follows the Gamma-Gamma distribution [13], [20].

2) The log-normal turbulence model

The Random process of the turbulence induced fading as a result of the influence of the weak atmospheric turbulence condition, can be modelled using the log-normal distribution function. This Log-normal turbulence model offers an opportunity to describe the weak atmospheric turbulence induced fading channel during the propagation of signal from the transmitter to the photodetector.

The Probability Density Function (PDF) that mathematically expresses the log-normal fading channel for an irradiance with log-normal Random Variable (RV), when $C_{mn} \geq 0$, is given as follows [5], [14], [35]:

$$f_{mn}(C_{mn}) = \frac{1}{(C_{mn}\sigma_I\sqrt{2\pi})} \exp(-\frac{(\ln(C_{mn}) + \frac{\sigma_I^2}{2})^2}{2\sigma_I^2}) \quad (19)$$

where *m = 1, 2 ..., M_T and n = 1, 2 ..., N_R.*

The variance parameter of the distribution used in this case is called the Rytov Variance which is denoted by the parameter σ_I^2, and it is expressed as follows [6]:

$$\sigma_I^2 = 1.23 C_n^2 k^{(7/6)} L^{(11/6)} \quad (20)$$

Under the weak scintillation theory, this Rytov Variance expression in (20) is mostly used when we assume a plane wave propagation. However, it can be said that the Rytov variance is proportional to the scintillation index. In the expression above showing the Rytov variance, the atmospheric turbulence strength or the refractive index parameter is represented using C_n^2. This parameter depends on the altitude of the optical link, and according to the atmospheric turbulence condition, it has a range that varies from 10^{-17} to 10^{-13} $m^{-2/3}$ [13], [14].

The expression for the normalized Log-irradiance variance also called the scintillation index (σ_s^2) is given as [13], [14]:

$$\sigma_s^2 = \exp(\psi_1 + \psi_2) - 1 \quad (21)$$

where parameters ψ_1 and ψ_2 respectively are given as [13]:

$$\psi_1 = \frac{(0.49\sigma_I^2)}{(1 + 0.18d^2 + 0.56\sigma_I^{12/5})^{7/6}} \quad (22)$$

$$\psi_1 = \frac{(0.51\sigma_I^2)}{(1 + 0.9d^2 + 0.62\sigma_I^{12/5})^{5/6}} \quad (23)$$

From the above expressions, we have the following parameters: the optical parameter, d, which is given as: $\sqrt{(kD^2)/4L}$, and also, the optical wave number, k, is given as: $2\pi/\lambda$. Where D represents the receiver aperture diameter of the Photodetector, the optical Link distance in meters is represented by L, and the optical wavelength in meters is denoted by λ.

III. Performance Analysis

A. Bit Error Rate Analysis for Log-normal Channel Model Using BPSK-SIM

Considering the same transmitted data symbols, that is, when the system allows the transmission of a data symbol '1', the Bit Error Rate (BER) can be derived as the probability of the output signal after demodulation to be less than zero $(R(t) < 0)$. Therefore, it can be said that the theoretical unconditional BER per subcarrier channel is given as [14], [35]:

$$P_e = \int_0^{\infty} P_{(e-i)}(C) f_c(C) dC \tag{24}$$

where $P_{(e-i)}(C)$ represents the instantaneous probability of error that is the same as the probability of obtaining $R(t) < 0$, whereby $R(t)$ is considered as a Gaussian random process that has an instantaneous mean given as $\frac{1}{4} C(t) P_p \Re \kappa A_c$ and a noise variance of σ_N^2. The parameter $f_c(C)$ represents the PDF of the random process which is as a result of the atmospheric scintillation within the system. Thus, the instantaneous error probability is given as [35]:

$$P_{(e-i)} = \frac{1}{\sqrt{2\pi}\sigma_N} \int_{-\infty}^{0} \exp\left[\frac{(R(t) - \frac{C P_p \Re \kappa A_c}{4})^2}{2\sigma_N^2}\right] dR \tag{25}$$

$$= Q\left(\frac{P_p \Re \kappa A_c}{4\sigma_N} \bullet C\right) \tag{26}$$

$$= Q\sqrt{\gamma} \tag{27}$$

where $Q(.)$ denotes the Gaussian Q-function and it is given as [35]:

$$Q(y) = \frac{1}{\sqrt{2\pi}} \int_y^{\infty} \exp(-t^2/2) dt \tag{28}$$

and the noise variance σ_N^2 at the input of the BPSK modulator is given as [35]:

$$\sigma_N^2 = 2qG^2 F_A \Re\left(\frac{\kappa}{4} P_p C\right) \Delta f + \left(4k_B \frac{T}{R_L}\right) F_N \Delta f \tag{29}$$

Also, $N_0 = 2\sigma_N^2$, such that N_0 represents the Noise Power Spectral Density (PSD) and where $q, G, F_A, T, \Delta f, F_N, k_B$ and R_L all represent the charge of the electron, average Avalanche Photo-Detector (APD) gain, additional noise factor, receiver noise temperature, effective noise bandwidth, noise figure of the amplifier, Boltzmann's constant and load resistance respectively.

During the weak atmospheric turbulence event in an FSO communication system, it is already a fact that the log-normal distribution perfectly describes the primary influence of turbulence $(C(t))$ which is identified as a random process [35]. The PDF $(f_c(C))$ for an FSO system described by a log-normal distribution can be expressed using the expression given in (19). The variance parameter σ_I^2 in this expression also represents the log-irradiance variance, which determines the strength of the atmospheric turbulence condition and it is a value that is dependent on the characteristics of the channel. This log-normal PDF continues to be valid for the Scintillation Index (S.I) which is given as [35]:

$$S.I = \sigma_s^2 = e^{\sigma_I^2} - 1. \tag{30}$$

Thus, using Eq. 30, the scintillation indices chosen for this research work were obtained from the selected log-irradiance variance values. These scintillation indices values are within the range of values that the log-normal model can handle. Therefore, we used these set of values to determine the minimum and maximum effects of weak atmospheric turbulence on the channels of the FSO communication links. Since the limit of the log-irradiance variance values that the log-normal model can handle for the weak atmospheric turbulence regime is 1.2 [6], thus, in this paper we chose to limit ourselves to log-irradiance variance values from 0.1 to 0.9.

The BER expression for the FSO system can be obtained by substituting (19) and (26) into (24), and this is shown below:

$$P_e = \int_0^{\infty} Q\left(\frac{P_p \Re \kappa A_c}{4\sigma_N} \bullet C\right) \times \frac{1}{\sqrt{2\pi}\sigma_I C} \exp\left[-\frac{(\ln(C) + \sigma_I^2/2)^2}{2\sigma_I^2}\right] dC \tag{31}$$

B. Average (Ergodic) Channel Capacity Analysis

1) Average Spectral Efficiency (ASE)

The Average Channel Capacity (ACC) is a very essential metric which can be used to determine or evaluate the optimal performance of the optical link. It can as well be used to determine the data rate that communicates between the available M-transmitter and N-photodetector. However, if the channel frequency response is known, and since the ACC is a system for obtaining the maximum achievable data rate, then we can also conveniently express the ACC of the systems in terms of the Average Spectral Efficiency (ASE) which will then be given in bits/seconds/Hertz [13], [14].

In the presence of weak atmospheric turbulences with fading strength less than one, the ACC can be derived analytically as shown in this section, for both the SISO-FSO link and the spatial diversity-FSO links including the $M_T \times N_R$ MIMO-FSO link.

The following assumptions were taken into consideration for this work in order to determine the ASE of the system:

(a). The optical channel of the FSO communication system is presumed to be tractable, stationary, ergodic with independent and identically distributed (i.i.d.) turbulence statistics and memoryless.

(b). A seamless (perfect) Channel State Information (CSI) is present at the M-transmitting optical lasers as well as at the N-receiving apertures [14].

Therefore, the ASE of the system can be expressed as follows [13], [14]:

$$\overline{C}_c = \frac{C_R}{B}(bits/s/Hz) = \int_{\Gamma} \log_2(1+\gamma) \times f_{\Gamma}(\Gamma) d\Gamma \quad (32)$$

where C_R is the channel's bit rate, B is the transmission bandwidth of the ergodic optical channel, γ denotes the total Signal to Noise Ratio (SNR) of the optical channels, $f_{\Gamma}(\Gamma)$ represents the joint Probability Density Function for the available array of optical channels present in the atmospheric turbulent regime and then the parameter Γ is a matrix representation of the MIMO atmospheric turbulence induced optical channels, and it is given as follows [5]:

$$\Gamma = \{\gamma_{mn}, m = 1, \cdots, M_T \;\; n = 1, \cdots, N_R\} \quad (33)$$

The expression in (32) above which can likewise be referred to as the ACC of the system is also defined as the ratio of the channel's bit rate (C_R) to the channel's bandwidth (B).

Since we have assumed that the channel is ergodic, therefore we can find the ergodic channel capacity for SISO, MISO, SIMO and MIMO as presented in the next sub-sections.

2) Ergodic channel capacity of MIMO-FSO channels

According to the arrangement of a MIMO system with multiple transmit M_T and receive N_R antennas, the channel will be represented by a matrix C which is given as $C \in \mathbb{C}^{M_T \times N_R}$. However, the transmitted and received signals can both be represented as vectors given as [36], [37]:

$$x \in \mathbb{C}^{M_T \times 1} \;\; and \;\; y \in \mathbb{C}^{N_R \times 1} \quad (34)$$

The symbol vector (x) for the transmitted signal consists of M_T unrelated input symbol vectors: $x_1, x_2, \cdots, x_{M_T}$. The received signal (y) can be expressed in matrix system as [36], [37]:

$$y = \sqrt{\frac{E_x}{M_T}} Cx + \nu_n \quad (35)$$

where E_x denotes the energy of the transmitted optical signal and ν_n is the noise vector and it is given as: $\nu_n = (\nu_{n_1}, \nu_{n_2}, \cdots, \nu_{n_{N_R}})^T \in C^{N_R - 1}$.

However, the capacity of a channel can be generally defined as follows [36], [37]:

$$C_c = \max_{f(x)} I(x:y) \; bits/channel\ use \quad (36)$$

where $f(x)$ is presented as the PDF of the transmitted optical signal vector (x) in consideration and the mutual information for both the transmit and received signal is represented with $I(x:y)$. Therefore, the capacity of a channel can be defined as the maximum mutual information obtained as a result of frequently changing the PDF of the transmitted optical signal vector.

Using the principle of information theory, the mutual information is given as [36]:

$$I(x:y) = \log_2 \det(I_{N_R} + \frac{E_x}{M_T N_0} C I_{M_T} C^H) bps/Hz \quad (37)$$

where the Hermitian symmetric matrix CC^H represents the channel matrix obtained from the auto-correlation matrix of the received signal y. I_{N_R} and I_{M_T} respectively represent the information about the receive and transmit antennas.

From (36) and (37), the channel capacity of a MIMO channel in cases where a deterministic MIMO channel is assumed, is given in bps/Hz as [36], [37]:

$$C_{c_{MIMO}} = \max_{M_T} \log_2 \det(I_{N_R} + \frac{E_x}{M_T N_0} C I_{M_T} C^H) \quad (38)$$

In cases where a random MIMO channel is assumed, thus, the channel matrix C is considered as a random matrix. Therefore, this suggest that the capacity of the MIMO channel is also obtained as randomly time-varying. As a result of this, the capacity of the MIMO channel can best be described using the time average. Since it is known that an ergodic process practically describes a random channel, then the ergodic channel capacity of a random MIMO channel is given in terms of expected value as [36], [37]:

$$\begin{aligned} \overline{C}_{c_{MIMO}} &= E\{C_{c_{MIMO}}\} \\ &= E\left\{ \max_{M_T} \log_2 \det(I_{N_R} + \frac{E_x}{M_T N_0} C I_{M_T} C^H) \right\} \end{aligned} \quad (39)$$

Thus, when CSI is available at the transmitter end, the ergodic channel capacity expression for the MIMO system is presented as shown in (39). However, when CSI is not available at the transmitter end, then the expression is simplified into the following [36], [37]:

$$\overline{C}_{c_{MIMO}} = E\left\{ \max_{M_T} \log_2(I_{N_R} + \frac{E_x}{M_T N_0} CC^H) \right\} \quad (40)$$

Meanwhile,

$$\|C\|_F^2 Tr(CC^H) = \sum_{i=1}^{M_T} \sum_{j=1}^{N_R} |c_{ij}|^2 \quad (41)$$

The FSO channel's total power gain is given as the squared Frobenius norm of the FSO-MIMO channel [36].

3) Ergodic channel capacity of SISO-FSO channels

For a SISO-FSO system that consists of a single transmit antenna M_T and a single receive antenna N_R, the received signal (y) can be written in linear form in terms of the transmitted signal x as:

$$y = \sqrt{\frac{E_x}{M_T}} Cx + \nu_n \quad (42)$$

where $M_T = 1$ and C represents the single FSO channel.

Thus, similarly to (38), the deterministic SISO channel capacity can be expressed as:

$$C_{c_{SISO}} = \max_{M_T} \log_2 \det(I_{N_R} + \frac{E_x}{M_T N_0} CI_{M_T} C^H) \quad (43)$$

In cases where maximum number of channel =*1*, $I_{M_T} = 1$ and $I_{N_R} = 1$, therefore, the ergodic channel capacity with Channel State Information (CSI) at the transmitter becomes [36]:

$$\overline{C}_{c_{SISO}} = E\{C_{c_{SISO}}\} = E\left\{ \log_2(1 + \frac{E_x}{M_T N_0} \|C\|_F^2) \right\} \quad (44)$$

Since $M_T = N_R = 1$, and where the channel's total power gain $\|C\|_F^2 = M_T = N_R$, then the ergodic channel capacity for a SISO channel in (44) becomes [36]:

$$\overline{C}_{c_{SISO}} = E\left\{ \log_2(1 + \frac{E_x}{N_0}) \right\} bps/Hz \quad (45)$$

Therefore, regardless of CSI available either at the transmitter and/or receiver sides, the channel capacity for SISO remains the same.

4) Ergodic channel capacity of SIMO-FSO and MISO-FSO channels

The SIMO channel to be described has a single M_T transmit antenna along with multiple N_R receive antennas. Since the channel gain can be expressed as $C \in \mathbb{C}^{N_R \times 1}$, then the time average of the channel capacity for SIMO system (regardless of CSI availability at the transmitter) is given in terms of the expected value as [36]:

$$\overline{C}_{c_{SIMO}} = E\{C_{c_{SIMO}}\} = E\left\{ \log_2(1 + \frac{E_x}{N_0} \|C\|_F^2) \right\} \quad (46)$$

where the channel's total power gain $\|C\|_F^2 = N_R$, then the ergodic SIMO channel capacity expression becomes:

$$\overline{C}_{c_{SIMO}} = E\left\{ \log_2(1 + \frac{E_x}{N_0} N_R) \right\} bps/Hz \quad (47)$$

However, for the ergodic MISO channel capacity, we have the following when CSI is not available at the transmitter, and when the channel gain is given as $C \in \mathbb{C}^{1 \times M_T}$ [36]:

$$\overline{C}_{c_{MISO}} = E\{C_{c_{MISO}}\} = E\left\{ \log_2(1 + \frac{E_x}{M_T N_0} \|C\|_F^2) \right\} \quad (48)$$

where $\|C\|_F^2 = M_T$, then the expression becomes:

$$\overline{C}_{c_{MISO}} = E\left\{ \log_2(1 + \frac{E_x}{N_0}) \right\} bps/Hz \quad (49)$$

Hence, it can be noticed that the ergodic channel capacity is the same for the SISO and MISO channels, if no CSI is available at the transmitter side.

Finally, if the transmitter side of the MISO channel has the CSI, then the expression becomes [36]:

$$\overline{C}_{c_{MISO}} = E\left\{ \log_2(1 + \frac{E_x}{N_0} M_T) \right\} bps/Hz \quad (50)$$

C. Outage Channel Capacity Analysis

The Outage Channel Capacity (OCC), ε, is an alternative statistical concept of the channel capacity which is defined in terms of the outage probability of the FSO systems. Therefore, to evaluate the OCC in terms of the rate of transmission $R(b/s/Hz)$, we can use the following outage probability expression [36]:

$$P_{out}(R) = P(C_C(C) < R\ bps/Hz) \quad (51)$$

whereby for the FSO MIMO channels we can say that $C_C(C) = C_{C_{MIMO}}$. Therefore, (51) becomes:

$$P_{out}(R) = P\left(\left\{ \max_{M_T} \log_2(I_{N_R} + \frac{E_x}{M_T N_0} CC^H \right\} < R \right) \quad (52)$$

In order words, the OCC can be defined as the maximum attainable data rate obtained when the outage probability as defined in (51) is less than the outage

channel capacity. It is required that the decoding error probability be made arbitrarily small in accordance with the rate of transmission R. However, in cases where this is not so, this suggests that the FSO system may experience an outage. Thus, the ergodic channel capacity of the spatial diversity FSO systems when there is no Channel State Information (CSI) at the transmitter end, is given in terms of the Cumulative Distribution Function (CDF).

IV. Performance Results and Discussion

In this section, as discussed earlier, the two various cases of weak atmospheric turbulence (i.e. mildly weak and moderately weak) analyzed in this paper are modelled using the Log-normal distribution model with BPSK signaling to provide a better performance. The analytical results obtained from the expressions derived in section 3 are used to make comparative studies on the performance analysis of the SISO and spatial diversity FSO systems in Log-normal fading. The analysis shows the evaluation of the BER, ACC and OCC for various atmospheric turbulence conditions of turbulence strength: $\sigma_I^2 = 0.1$ and $\sigma_I^2 = 0.9$ for respective cases of mildly weak and moderately weak atmospheric turbulence regimes. Here, the diameter of the Photo-detector's receiver aperture was taken to be *10 cm*, the optical wavelength $\lambda = 850$ *nm*, responsivity of the photo-detector $\Re = 1$ and for the range of the atmospheric turbulence links we chose distances of *2 km, 4 km and 6 km*.

A. BER Performance Results

Table I shows the input parameters used for obtaining the BER for the FSO systems considered. The predicted and calculated BER performance as derived in (31) against the Signal to Noise ratio in dB for SISO ("non-diversity") and spatial diversity schemes employing the BPSK-SIM through the weak atmospheric turbulence induced channels is illustrated in Fig. 3. The log-irradiance variance values of $\sigma_I^2 = \{0.1$ and $0.9\}$ were considered for the log-normal fading channels and also an ideal channel (with no atmospheric turbulence) was used as a benchmark for the performance analysis.

TABLE I: INPUT PARAMETERS

Parameter	Value
Operating Wavelength	850 nm
Rytov Variance Values	at 0.1 and 0.9
Photodetector Responsivity	1
Refractive Index	$9\times10^{-16}m^{-2/3}$
Irradiance	0.01 to 5 (500 samples)
Modulation Index	1
Subcarrier Signal Amplitude	1

To achieve a better system performance, we need to achieve Bit Error probability with values as low as the order of 10^{-9} or less. Fig. 3 shows the BER performance of various FSO spatial diversity channels from the less complex ones (such as 1×2 and 2×2 systems) up to very high-order MIMO systems (such as 4×4, 6×6 and 8×8 MIMO systems) as a function of the SNR, for two various values of atmospheric turbulence strength (i.e. $\sigma_I^2 = 0.1$ and $\sigma_I^2 = 0.9$) representing the mildly weak and moderately weak atmospheric turbulence regimes respectively. The performance of the "non-diversity" FSO system (SISO) is also included in the analysis shown in Fig. 3 for the purpose of comparison and as a benchmark to measure the diversity gain of the BER or SNR. The performance analysis as clearly observed from the figure, shows significant improvement as number of the transmit lasers and receive photo-detectors increases in a certain order, but more significantly for FSO systems with higher-order antenna configurations such as the 6×6 and 8×8 MIMO systems. More explicitly, a significant BER performance degradation results from an increase in the strength of the atmospheric turbulence from $\sigma_I^2 = 0.1$ to $\sigma_I^2 = 0.9$. On the other hand, this performance degradation becomes absolutely insignificant when the 8×8 MIMO system is used, since at BER of 10^{-9}, the SNR required by the 8×8 MIMO system is approximately the same for both the mildly weak and moderately weak atmospheric turbulence regimes. Thus, as expected, as the order of the spatial diversity increases from the "non-diversity" case $(M = N = 1)$ to higher-order diversity case $(M = N = 8)$, the BER decreases significantly. Also, in order to reach a BER of 10^{-9}, it was noticed that the required SNR decreased by approximately 28 dB, 31 dB and 35 dB, as the system increases from the "non-diversity" FSO system to 4×4, 6×6 and 8×8 MIMO systems respectively at $\sigma_I^2 = 0.9$. Therefore, this analysis has shown the various influence of the Log-irradiance variance value (σ_I^2) on the BER performance of various antenna-order configurations of the FSO system. On the other hand, the AWGN channel (no turbulence channel) can also be used as a benchmark to determine the required SNR loss. From the results in Fig. 3, we observed that in the non-atmospheric turbulence regime, the required SNR is approximately 16 dB over the AWGN channel at a BER of 10^{-9}, thus, the required SNR loss is approximately 2.4 dB, 1.4 dB, 1 dB and 0 dB for the 1×8, 4×4, 6×6 and 8×8 diversity systems to attain similar BER in the mildly weak atmospheric turbulence regime at $\sigma_I^2 = 0.1$. But at that same BER, the SNR loss is 11.5 dB, 7 dB, 3.75 dB and 0.1 dB for the 1×8, 4×4, 6×6 and 8×8 diversity systems under a moderately weak atmospheric turbulence regime at $\sigma_I^2 = 0.9$. However, the 8×8 MIMO system possesses no significant SNR loss at both $\sigma_I^2 = 0.1$ and 0.9, since

the required SNR is still approximately 16 dB at the same BER of 10^{-9}.

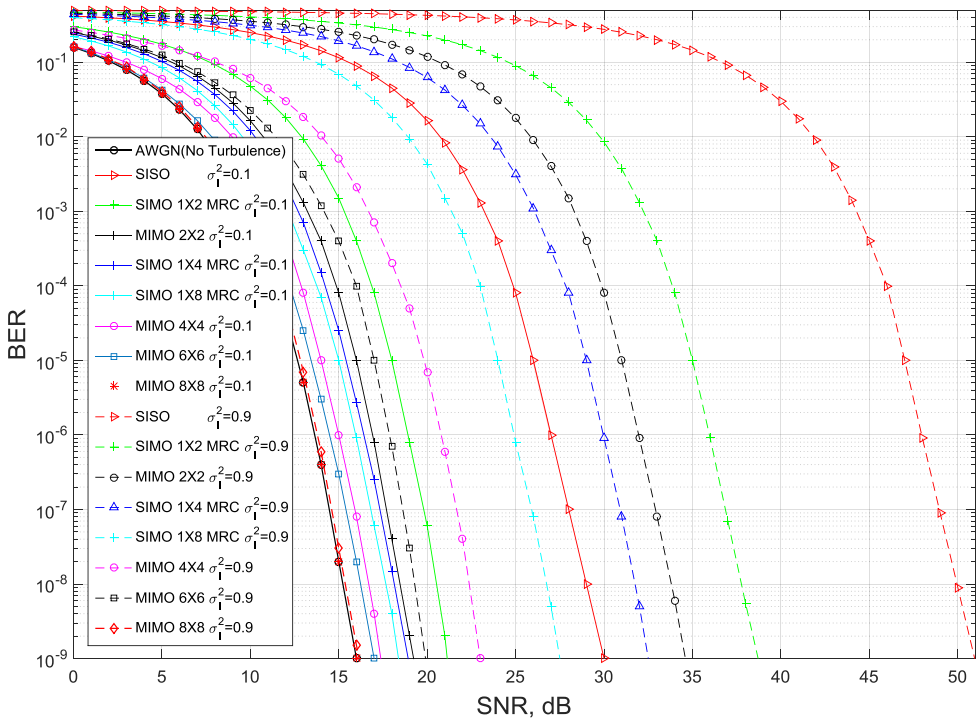

Fig. 3. BER performance against the SNR for the FSO-SISO and FSO-Spatial diversity schemes of SIMO and MIMO in log-normal channel for $\sigma_I^2 = 0.1$ and $\sigma_I^2 = 0.9$.

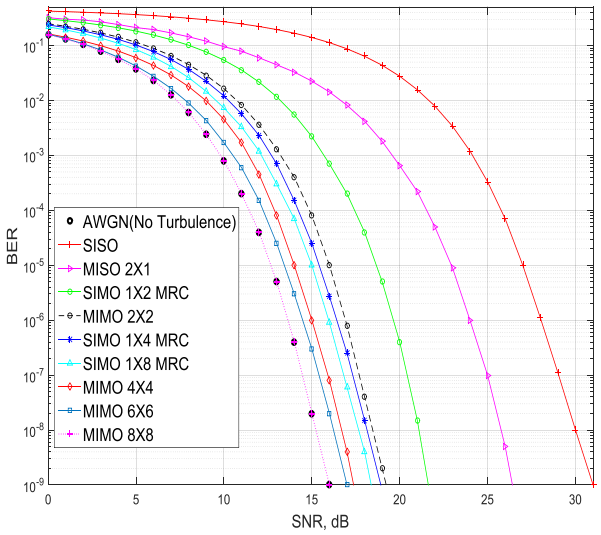

Fig. 4. BER performance against the SNR for FSO-SISO and FSO-Spatial diversity schemes of SIMO, MISO and MIMO in log-normal channel with refractive index $C_n^2 = 9\times10^{-16}\ m^{-2/3}$ for distance *L = 2000 m.*

Figs. 4, 5 and 6 show the BER performance analysis of various FSO spatial diversity channels from the single-order (SISO) FSO system up to very high-order MIMO FSO systems (such as 4×4, 6×6 and 8×8 MIMO systems) as a function of the SNR, for atmospheric turbulence strength parameter of $C_n^2 = 9\times10^{-16}\ m^{-2/3}$, representing the weak atmospheric turbulence regime, with three diverse optical link distances (i.e. *2 km, 4 km* and *6 km*). These figures depict the influence of the various optical link distances over the BER performance of various antenna order configurations of the spatial diversity FSO system.

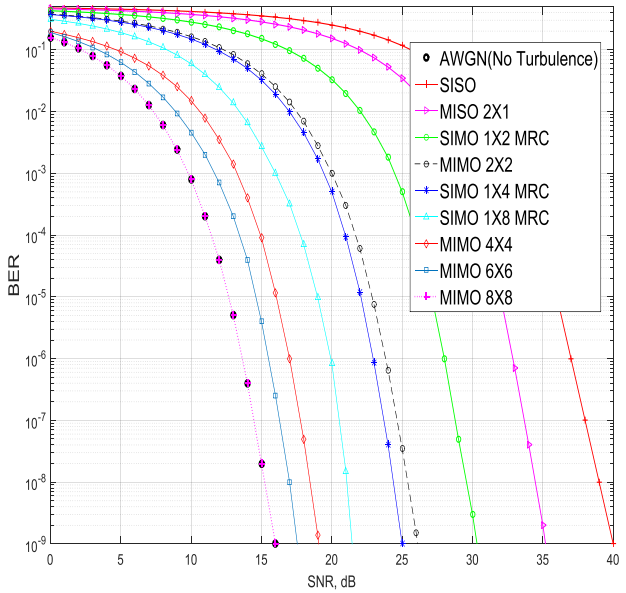

Fig. 5. BER performance against the SNR for FSO-SISO and FSO-Spatial diversity schemes of SIMO, MISO and MIMO in log-normal channel with refractive index $C_n^2 = 9\times10^{-16}\ m^{-2/3}$ for distance *L = 4000 m.*

From Fig. 4, the BER performance analysis for the SISO-FSO, MISO-FSO, SIMO-FSO and the MIMO-FSO systems over the Log-normal fading channel with

refractive index $C_n^2 = 9\times10^{-16}\ m^{-2/3}$ and distance $L = 2000\ m$ is illustrated. Fig. 4 shows that at this atmospheric turbulence strength parameter and the optical link distance, the antenna order of the spatial diversity system strongly determines the systems' performance. For instance, in order to achieve a BER of 10^{-9}, an improvement was observed in terms of SNR gain of 12.6 *dB*, 13.6 *dB*, 14 *dB* and 15 *dB* for 1×8, 4×4, 6×6, and 8×8 FSO spatial diversity systems respectively when compared to the "non-diversity" system. However, at an optical link distance of 2 *km*, no SNR loss was observed on the 8×8 MIMO system when compared to the AWGN channel at a BER of 10^{-9}.

Fig. 5 shows that at atmospheric turbulence strength parameter $C_n^2 = 9\times10^{-16}\ m^{-2/3}$ and optical link distance $L = 4000\ m$, there exist a reduction in the required SNR of ≈ 18.5 *dB*, 21 *dB*, 22.5 *dB* and 24 *dB* for 1×8, 4×4, 6×6, and 8×8 FSO spatial diversity systems respectively when compared to the "non-diversity" system in order to attain the BER of 10^{-9}. Also, at this optical link distance, no SNR loss was observed on the 8×8 MIMO system when compared to the AWGN channel at a BER of 10^{-9}.

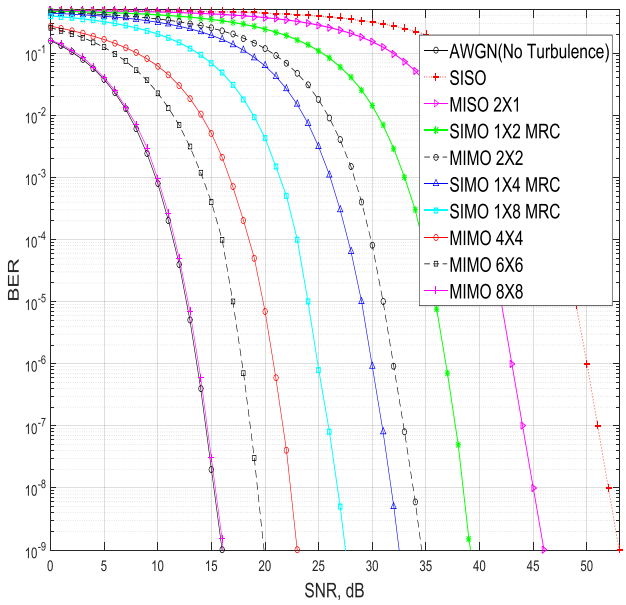

Fig. 6. BER performance against the SNR for FSO-SISO and FSO-Spatial diversity schemes of SIMO, MISO and MIMO in log-normal channel with refractive index $C_n^2 = 9\times10^{-16}\ m^{-2/3}$ for distance *L = 6000 m.*

Fig. 6 shows that at the atmospheric turbulence strength parameter $C_n^2 = 9\times10^{-16}\ m^{-2/3}$ and the optical link distance $L = 6000m$, the 1×8, 4×4, 6×6 and 8×8 spatial diversity FSO systems, requires an additional SNR to reach the BER of 10^{-9}, when they are all compared with the AWGN channel (no turbulence channel) as the benchmark. The SNR penalties for these four (4) higher-order FSO systems are *11.5 dB, 7 dB, 3.75 dB and 0.1 dB* respectively at a distance $L = 6000m$ when compared to the AWGN channel.

However, in order to achieve the same BER, an improvement was observed in terms of SNR gain of *25.5 dB, 30 dB, 33.25 dB and 36.9 dB* for 1×8, 4×4, 6×6, and 8×8 FSO spatial diversity systems respectively when compared to the "non-diversity" system. Moreover, at an optical link distance of 6 *km*, no significant SNR loss was observed on the 8×8 MIMO system when compared to the AWGN channel at a BER of 10^{-9}.

B. Average Ergodic Channel Capacity Results

Fig. 7 and Fig. 8 illustrate the Average Ergodic Channel Capacity for various groupings of transmitters (M_T) and receivers (N_R) in the presence of the weak atmospheric turbulence conditions. The various combinations of M_T and N_R are considered under the two log-irradiance variance values of $\sigma_I^2 = \{0.1$ and $0.9\}$. The calculated Average Ergodic Channel Capacity as derived from (32) to (50), against the Signal to Noise Ratio in dB for SISO ("non-diversity") and spatial diversity schemes through the weak atmospheric turbulence induced channels are illustrated in these figures. The ASE for SISO-FSO, MISO-FSO, SIMO-FSO and MIMO-FSO channels with respect to the SNR (γ), over the two different values of the log-irradiance variance were determined and analyzed.

Fig. 7 shows the ACC of diverse FSO spatial diversity channels with the same number of transmit and receive antennas (i.e. $M_T = N_R$) as a function of the SNR, for two different values of atmospheric turbulence strength (i.e. $\sigma_I^2 = \{0.1$ and $0.9\}$) representing the mildly weak and moderately weak turbulence regimes respectively. It was observed from this illustration that the ASE which suggests the bandwidth efficiency of the FSO systems depends strongly on the changes in the strength of the atmospheric turbulence. Fig. 7 illustrates that irrespective of the influence of atmospheric turbulence on the ASE, the higher-order MIMO systems will still provide a significant bandwidth efficiency on the FSO system. However, it can be vividly noticed that the influence of atmospheric turbulence becomes significant on the "non-diversity" systems. This results into the fact that as the turbulence increases, there can arise a time whereby the bandwidth efficiency of the "non-diversity" system will approach a value close to zero or actually becomes zero. On the other hand, it can be noticed that 8×8 MIMO systems gives the same ACC for both the mildly weak and moderately weak atmospheric turbulence regimes. It is worth mentioning that an 8×8 MIMO system is

unaffected by the level of turbulence within the range of the weak atmospheric turbulence regime, whereby at SNR of 30 *dB* it yields a bandwidth efficiency of up to 71 *bps/Hz*. Using the "non-diversity" FSO system as the benchmark, at SNR of 30 *dB*, we noticed a bandwidth efficiency gain of ≈ 63 *bps/Hz*, 45 *bps/Hz*, 27 *bps/Hz* and 8 *bps/Hz* for 8×8, 6×6, 4×4 and 2×2 MIMO systems respectively at $\sigma_I^2 = 0.9$.

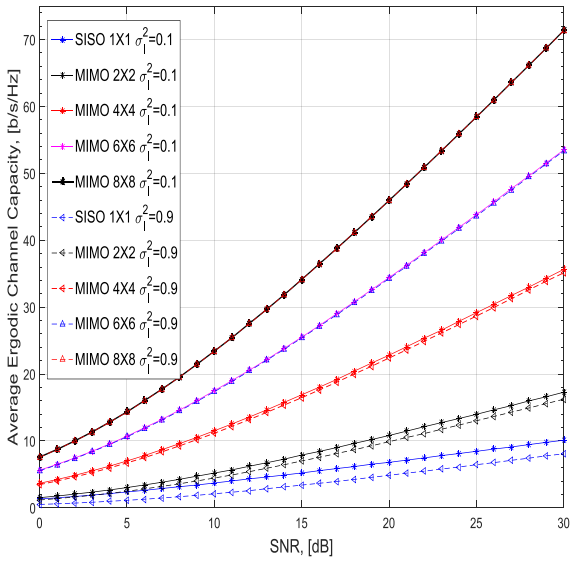

Fig. 7. Ergodic channel capacity analysis for FSO-SISO and FSO-Spatial diversity systems over a log-normal channel with $\sigma_I^2 = 0.1$ and $\sigma_I^2 = 0.9$.

Fig. 8 shows the ACC of diverse FSO spatial diversity channels with the different number of transmit and receive antennas (i.e. $M_T \neq N_R$) as a function of the SNR, for atmospheric turbulence strength $\sigma_I^2 = 0.9$ representing the moderately weak turbulence regime. This explains the disparity in the Average (Ergodic) Channel Capacity of the transmit diversity against the receive diversity with MRC technique. Also in this figure, using the "non-diversity" system as the benchmark, at $\sigma_I^2 = 0.9$, we deduced that the bandwidth efficiency provided by the receive diversity systems with MRC technique is far greater than that obtained from the transmit diversity. As the order of the spatial diversity increases, a tremendous increase in ACC was noticed. This suggests that the higher-order SIMO spatial diversity systems provide significant improvement to the ACC. Therefore, using the "non-diversity" FSO system as the benchmark, at SNR of 30 *dB*, we noticed that the ACC gain was approximately 1 *bps/Hz* for 8×1 transmit diversity FSO system, while it extends up to ≈ 24 *bps/Hz*, 16 *bps/Hz*, 8 *bps/Hz* and 6.5 *bps/Hz* for 1×8, 1×6, 1×4 and 1×2 receive diversity FSO systems respectively.

Therefore, from Figs. 7 and 8, it can be noticed that channel performance improves only if there is an increase in the number of transmit and receive antennas. But this is greatly noticed when there is an increase in the receive antennas, suggesting that the MIMO and SIMO FSO systems provide a better channel performance than the SISO and MISO FSO systems considered. However, from the analysis, it is clearly noticed that the ACC depends strongly on the strength of the atmospheric turbulence which determines the log-irradiance variance value. As the log irradiance variance values increases, the ACC of the considered systems reduces.

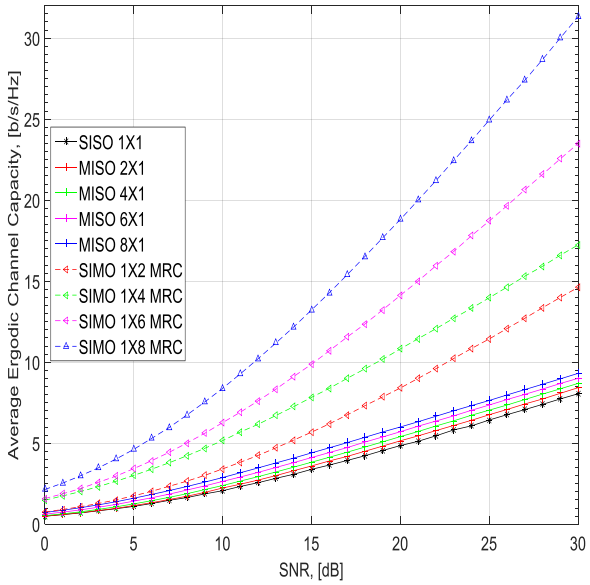

Fig. 8. Ergodic Channel Capacity analysis for transmit and receive FSO-Spatial diversity systems over a log-normal channel with $\sigma_I^2 = 0.9$.

C. Outage Probability Results

The CDFs of the channel capacities for the spatial diversity FSO systems under the Log-normal fading are illustrated in Figs. 9 and 10 when the SNR is 10 *dB* and 20 *dB* respectively, at optical link distance L = 6 *km*, optical wavelength $\lambda = 850$ *nm* and the atmospheric turbulence strength $C_n^2 = 9\times 10^{-16}$ $m^{-2/3}$. Fig. 9 illustrates the CDF of some spatial diversity FSO systems as a function of the transmission rate *R*, at SNR of 10 *dB*, optical link distance L = 6 *km* and under a weak turbulence condition of atmospheric turbulence strength $C_n^2 = 9\times 10^{-16}$ $m^{-2/3}$. At the indicated OCC of $\varepsilon = 0.1$, it can be observed that the higher-order spatial diversity systems yields significant data rate of ≈ 5.25 *b/s/Hz*, 7 *b/s/Hz*, 11.3 *b/s/Hz*, 11.6 *b/s/Hz* and 15.5 *b/s/Hz* for 2×4, 4×4, 6×6, 4×8 and 8×8 MIMO FSO systems. However, it can also be noticed that the 4×8 and 6×6 MIMO FSO systems have almost the same data rate at $\varepsilon = 0.1$ when the SNR is 10 *dB*, despite the difference in their antenna order configurations. In contrast, as expected, the "non-diversity" FSO system (SISO) shows no significant improvement in its channel capacity unlike the spatial diversity FSO systems.

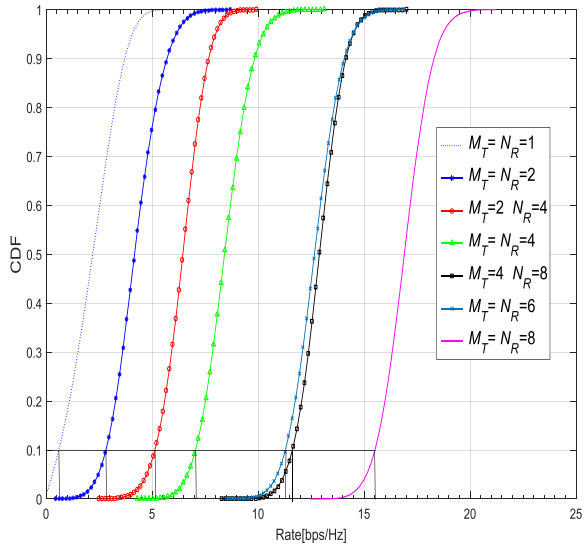

Fig. 9. Cumulative Distribution Function of the FSO-SISO and FSO-Spatial diversity channel capacities as a function of the transmission rate over a Log-normal channel with $C_n^2 = 9\times10^{-16}\, m^{-2/3}$, at SNR = 10 *dB* and distance L = 6 *km*.

Fig. 10 illustrates the CDF of some spatial diversity FSO systems as a function of the transmission rate *R*, at SNR of 20 *dB*, optical link distance L = 6 *km* and under atmospheric turbulence strength $C_n^2 = 9\times10^{-16}\, m^{-2/3}$. At the indicated OCC of $\varepsilon = 0.1$, the data transmission rate of the higher-order spatial diversity systems are ≈ 11 *b/s/Hz*, 16.5 *b/s/Hz*, 24 *b/s/Hz*, 26 *b/s/Hz* and 35.5 *b/s/Hz* for 2×4, 4×4, 4×8, 6×6 and 8×8 MIMO FSO systems, while the "non-diversity" FSO system yields a data rate of 2.5 *b/s/Hz*.

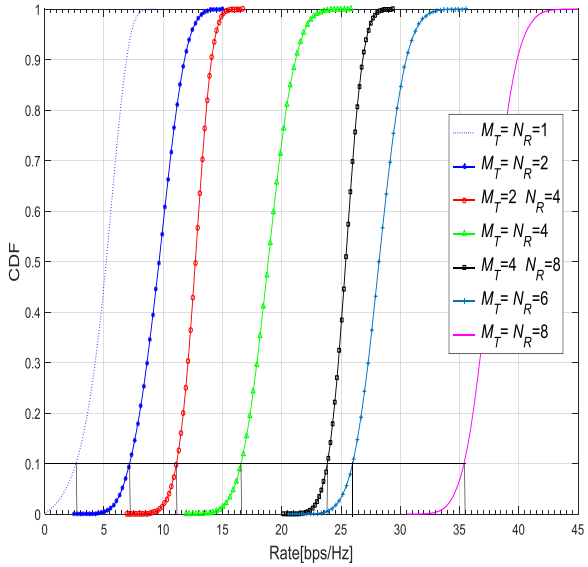

Fig. 10. Cumulative Distribution Function of the FSO-SISO and FSO-Spatial diversity channel capacities as a function of the transmission rate over a Log-normal channel with $C_n^2 = 9\times10^{-16}\, m^{-2/3}$, at SNR = 20 *dB* and distance L = 6 *km*.

However, when the SNR is 20 *dB*, one of the notable facts is that at $\varepsilon = 0.1$, the CDF of the 4×8 and 6×6 MIMO systems are not quite close unlike the CDF at SNR = 10 *dB*. The 6×6 MIMO system has a data rate gain of about 2 *b/s/Hz* over the 4×8 MIMO system when the SNR increases from 10 *dB* to 20 *dB*. This can also be as a result of the fact that the number of channels of the 6×6 MIMO system is greater than that of the 4×8 MIMO system. Thus, these two figures (9 and 10) have shown that channel capacities of the higher-order spatial diversity FSO systems improve optimally as the number of the transmit antennas and receive antennas increases.

V. Conclusion

The optical SISO and spatial diversity systems employing the BPSK-SIM across optical sources with Coherent Detection over the Log-normal model for weak atmospheric turbulence condition, with two chosen scintillation indices have been analyzed. The two scintillation indices for this analysis were given in terms of the log-irradiance variance values of $\sigma_I^2 = 0.1$ and $\sigma_I^2 = 0.9$, respectively representing mildly weak and moderately weak atmospheric turbulence conditions. The analyses made in this report were necessary for observing the best performance improvement that can ever be obtained from higher-order spatial diversity systems for Free Space Optical communications. This knowledge can be used to avoid reduction in transmission capacity as well as any possible outages. However, according to the results of the BER performance analysis for all the scenarios considered, it was observed that the SNR (dB) needed to obtain an optimal BER increases along with the increase in the atmospheric turbulence level which is indicated by the scintillation indices. Among the higher-order spatial diversity systems that were considered under the weak atmospheric turbulence regime, 8×8 MIMO system gave the optimum BER and channel capacity performances.

Therefore, the efficiency and power of the higher-order spatial diversity system especially the 8×8 MIMO system was established in the presence of weak atmospheric turbulence and considered for average BER of 10^{-9}. As a matter of fact, it is important to note that as the spatial diversity antenna order configuration increases, there exist a practical complexity limitation introduced into the system. This practical limitation is as a result of the complexities of the higher-order spatial diversity techniques with higher number of transmit and receive antennas involved in the build-up of the FSO communication system design. This makes it complicated in the practical sense. This form of advance spatial diversity techniques has been suggested to provide improvement on the system performance in FSO communications when considering relatively severe scintillation channels.

Thus, when implementation is not focused on the complexity of the design, higher-order spatial diversity techniques and BPSK-SIM can be employed in FSO

communications through channels that are induced by atmospheric turbulence. This results into improving the FSO link performance as well as to reduce transmission power.

ACKNOWLEDGMENT

One of the authors of this paper hereby wishes to acknowledge the financial support of the University of KwaZulu-Natal, Durban, South Africa, towards his on-going PhD.

REFERENCES

[1] E. Bayaki, R. Schober, and R. K. Mallik, "Performance analysis of MIMO free-space optical systems in gamma-gamma fading," *IEEE Transactions on Communications*, vol. 57, no. 11, pp. 3415–3424, 2009.

[2] K. Prabu and D. S. Kumar, "BER analysis of DPSK–SIM over MIMO free space optical links with misalignment," *Optik-International Journal for Light and Electron Optics*, vol. 125, no. 18, pp. 5176–5180, 2014.

[3] S. M. Aghajanzadeh and M. Uysal, "Diversity–multiplexing trade-off in coherent free-space optical systems with multiple receivers," *Journal of Optical Communications and Networking*, vol. 2, no. 12, pp. 1087–1094, 2010.

[4] X. Zhu and J. M. Kahn, "Free-space optical communication through atmospheric turbulence channels," *IEEE Transactions on Communications*, vol. 50, no. 8, pp. 1293–1300, 2002.

[5] T. H. Duyen and A. T. Pham, "Performance analysis of MIMO/FSO systems using SC-QAM signaling over atmospheric turbulence channels," *IEICE Transactions on Fundamentals of Electronics, Communications and Computer Sciences*, vol. 97, no. 1, pp. 49–56, 2014.

[6] X. Tang, S. Rajbhandari, W. O. Popoola, Z. Ghassemlooy, E. Leitgeb, S. S. Muhammad, and G. Kandus, "Performance of BPSK subcarrier intensity modulation free-space optical communications using a log-normal atmospheric turbulence model," in *Proc. Symposium on Photonics and Optoelectronic*, 2010, pp. 1–4.

[7] M. Ijaz, Z. Ghassemlooy, H. L. Minh, S. Rajbhandari, and J. Perez, "Analysis of fog and smoke attenuation in a free space optical communication link under controlled laboratory conditions," in *Proc. International Workshop on Optical Wireless Communications*, 2012, pp. 1–3.

[8] Y. Gao, M. Wu, and W. Du, "Performance research of modulation for optical wireless communication system," *Journal of Networks*, vol. 6, no. 8, pp. 1099–1105, 2011.

[9] J. Park, E. Lee, and G. Yoon, "Average bit-error rate of the Alamouti scheme in gamma-gamma fading channels," *Photonics Technology Letters*, vol. 23, no. 4, pp. 269–271, 2011.

[10] B. Barua and D. Barua, "Evaluate the performance of FSO communication link with different modulation technique under turbulent condition," in *Proc. 14th International Conference on Computer and Information Technology*, 2011, pp. 191–195.

[11] A. Garcıa-Zambrana, C. Castillo-V ´azquez, and B. Castillo-V´azquez, "On the capacity of FSO links over gamma-gamma atmospheric turbulence channels using OOK signaling," *EURASIP Journal on Wireless Communications and Networking*, p. 64, 2010.

[12] O. A. Layioye, T. J. O. Afullo, and P. A. Owolawi, "Variation of altitude on the variance of angle of arrival fluctuations for beam propagation in free space optical communications," in *Proc. 3rd IEEE International Conference on Advances in Computing Communication and Engineering*, 2016, pp. 120-125.

[13] H. D. Trung, D. H. Ai, and A. T. Pham, "Average channel capacity of free-space optical MIMO systems over atmospheric turbulence channels," *The University of Aizu Aizuwakamatsu-shi*, Fukushima, Japan, 2014, pp. 965–8580.

[14] H. D. Trung, B. T. Vu, and A. T. Pham, "Performance of free space optical MIMO systems using SC-QAM over atmospheric turbulence channels," in *Proc. IEEE International Conference on Communications*, 2013, pp. 3846–3850.

[15] S. Zvanovec, J. Perez, Z. Ghassemlooy, S. Rajbhandari, and J. Libich, "Route diversity analyses for free-space optical wireless links within turbulent scenarios," *Optics Express*, vol. 21, no. 6, pp. 7641–7650, 2013.

[16] B. Barua and D. Barua, "Channel capacity of MIMO FSO system under strong turbulent condition," *IJECS-IJENS*, vol. 11, no. 2, 2011.

[17] J. Li, J. Q. Liu, and D. P. Taylor, "Optical communication using subcarrier PSK intensity modulation through atmospheric turbulence channels," *IEEE Transactions on Communications*, vol. 55, no. 8, pp. 1598–1606, 2007.

[18] C. Abou-Rjeily, "On the optimality of the selection transmit diversity for MIMO-FSO links with feedback," *Communications Letters, IEEE*, vol. 15, no. 6, pp. 641–643, 2011.

[19] E. Bayaki and R. Schober, "Performance and design of coherent and differential space-time coded FSO systems," *Journal of Lightwave Technology*, vol. 30, no. 11, pp. 1569–1577, 2012.

[20] O. A. Layioye, T. J. O. Afullo, and P. A. Owolawi, "Calculations of the influence of diverse atmospheric turbulence conditions on free space optical communication system using BPSK-SIM over the gamma-gamma model," in *Proc. South Africa Telecommunications Networks and Applications Conference*, Western Cape, South Africa, 2016, pp. 362-367.

[21] Z. Chen, S. Yu, T. Wang, G. Wu, H. Guo, and W. Gu, "Spatial correlation for transmitters in spatial MIMO optical wireless links with gaussian-beam waves and aperture effects," *Optics Communications*, vol. 287, pp. 12–18, 2013.

[22] J. Zhang, L. Dai, Y. Han, Y. Zhang, and Z. Wang, "On the ergodic capacity of MIMO free-space optical systems over turbulence channels," *IEEE Journal on Selected Areas in Communications*, vol. 33, no. 9, pp. 1925–1934, 2015.

[23] K. P. Peppas and P. T. Mathiopoulos, "Free-Space optical communication with spatial modulation and coherent

detection over HK atmospheric turbulence channels," *Journal of Lightwave Technology*, vol. 33, no. 20, pp. 4221–4232, 2015.
[24] M. Safari and S. Hranilovic, "Diversity and multiplexing for near-field atmospheric optical communication," *IEEE Transactions on Communications*, vol. 61, no. 5, pp. 1988–1997, 2013.
[25] W. O. Popoola and Z. Ghassemlooy, "BPSK subcarrier intensity modulated free-space optical communications in atmospheric turbulence," *Journal of Lightwave Technology*, vol. 27, no. 8, pp. 967–973, 2009.
[26] S. M. Haas and J. H. Shapiro, "Capacity of wireless optical communications," *IEEE Journal on Selected Areas in Communications*, vol. 21, no. 8, pp. 1346–1357, 2003.
[27] E. J. Lee and V. W. S. Chan, "Diversity coherent receivers for optical communication over the clear turbulent atmosphere," in *Proc. International Conference on Communications*, 2007, pp. 2485–2492.
[28] X. Song, M. Niu, and J. Cheng, "Error rate of subcarrier intensity modulations for wireless optical communications," *Communications Letters*, vol. 16, no. 4, pp. 540–543, 2012.
[29] A. T. Pham, T. C. Thang, S. Guo, and Z. Cheng, "Performance bounds for turbo-coded SC-PSK/FSO communications over strong turbulence channels," in *Proc. International Conference on Advanced Technologies for Communications*, 2011, pp. 161–164.
[30] S. G. Wilson, M. Brandt-Pearce, M. Baedke, and Q. Cao, "Optical MIMO transmission with multipulse PPM," in *Proc. International Symposium on Information Theory*, 2004, p. 289.
[31] S. G. Wilson, M. Brandt-Pearce, Q. Cao, and J. H. Leveque III, "Free-Space optical MIMO transmission with Q-ary PPM," *IEEE Transactions on Communications*, vol. 53, no. 8, pp. 1402–1412, 2005.
[32] S. G. Wilson, M. Brandt-Pearce, Q. Cao, and M. Baedke, "Optical repetition MIMO transmission with multipulse PPM," *IEEE Journal on Selected Areas in Communications*, vol. 23, no. 9, pp. 1901–1910, 2005.
[33] D. A. Luong and A. T. Pham, "Average capacity of MIMO free-space optical gamma-gamma fading channel," in *Proc. IEEE International Conference on Communications*, 2014, pp. 3354–3358.
[34] C. E. Shannon, "A mathematical theory of communication," *ACM SIGMOBILE Mobile Computing and Communications Review*, vol. 5, no. 1, pp. 3–55, 2001.
[35] D. A. Luong, C. T. Truong, and A. T. Pham, "Effect of APD and thermal noises on the performance of SC-BPSK/FSO systems over turbulence channels," in *Proc. 18th Asia-Pacific Conference on Communications*, 2012, pp. 344–349.
[36] Y. S. Cho, J. Kim, W. Y. Yang, and C. G. Kang, *MIMO-OFDM Wireless Communications with MATLAB*, John Wiley & Sons, 2010.
[37] K. D. Rao, *Channel Coding Techniques for Wireless Communications*, Springer, 2015.

Okikiade A. Layioye received his B. Tech degree in Physics (with Electronics) from the Federal University of Technology, Akure, in 2008. He holds a Masters degree in Electronic Communications and Computer Engineering from the University of Nottingham, England, United Kingdom in 2012. He is currently a PhD student at the University of KwaZulu-Natal, Durban, South Africa. His research interests are in optical communications, wireless communications, telecommunications engineering and electronic communications.

Thomas J. O. Afullo is a Professor of Electronic Engineering and he was the former Discipline Academic Leader of the School of Electrical, Electronic and Computer Engineering at the University of KwaZulu-Natal, Durban, South Africa. He has about 36 years working experience in the Telecommunications industry and academia. His research interests are in modeling of radio wave propagation, telecommunications engineering, wireless networks and power line communications.

Pius A. Owolawi is a professor and HOD of the Department of Computer Engineering at Tshwane University of Technology, Pretoria, South Africa. He received his B.Tech degree in Physics/Electronics from the Federal University of Technology, Akure, in 2001. He obtained an MSc and PhD degrees in Electronic Engineering from the University of KwaZulu-Natal in 2006 and 2010, respectively. His research interests are in the modeling of radio wave propagation, fiber optic communication, radio planning and optimization techniques.

